Life Science Informatics Publications

Research Journal of Life Sciences, Bioinformatics, Pharmaceutical and Chemical Sciences

Journal Home page http://www.rjlbpcs.com/

RJLBPCS

ISSN 2454-6348

Original Research Article **DOI: 10.26479/2024.1004.03**

MOLECULAR DOCKING STUDIES ON THERAPEUTIC AGENTS FOR COVID 19 CORONAVIRUS INFECTION- A NOVEL APPROACH TO ITS TREATMENT

Shyamalambica Peri*

Vignan Institute of Pharmaceutical Technology, Duvvada, Andhra Pradesh, India.

ABSTRACT: The novel coronavirus disease (COVID-19) is caused by SARS-CoV-2, which affects the respiratory system. The first case of the Covid 19 was detected in December in China. Later, it spread all over the world. There are few vaccinations for COVID-19, but drugs are unavailable for the disease. As a result, demands for the innovation of more effective viral drugs have emerged. The present study is directed towards finding inhibitors against the Non-structural protein 2, which is essential and plays a role in the modulation of host cell survival signaling pathway by interacting with the host prohibitin proteins; these proteins play a role in maintaining the functional integrity of the mitochondria and also protects the cells from the stress. The structure of the biological target was used to predict candidate drugs that could bind with high affinity and selectivity to the target. The ProtParam calculates the primary features of the protein. The three-dimensional structure of the non-structural protein is constructed using the homology modeling tool MODELER, which utilizes several available non-structural protein structures as templates. The structure is then subjected to deep optimization and validated by the structure validation tools PROCHECK and VERIFY3D. The CASTp server was used to analyze the receptor's active sites in molecular binding. This predicted structure of Nonstructural protein will serve as the future development of effective inhibitors with potential natural drugs.

Keywords: Novel coronavirus, Non-structural protein 2, Homology modeling, ligands.

Article History: Received: July 28, 2024; Revised: August 14, 2024; Accepted: August 28, 2024.

Corresponding Author: Shyamalambica Peri*

Vignan Institute of Pharmaceutical Technology, Duvvada, Andhra Pradesh

Email Address: s.ambica.peri90@gmail.com

1.INTRODUCTION

Coronavirus (COVID-19) is a respiratory infectious disease caused by the newly discovered coronavirus. It spreads primarily through droplet infection (saliva or discharge from the infected person). The symptoms of the disease are shortness of breath, fever, cough, and cold. This disease also shows other symptoms like loss of smell, fatigue, abdominal pain, diarrhea, and muscle aches. It primarily affects older people and those with medical problems like cancer, chronic respiratory disease, diabetes, and cardiovascular disease. The single-stranded RNA virus that causes the novel coronavirus disease is a virus strain of severe acute respiratory syndrome coronavirus 2 (SARS-CoV-2). The first onset of the disease was detected in Wuhan, China, in December 2019. Afterword's total confirmed cases, 12768307 confirmed COVID-19 cases were reported, and 566654 deaths by 13 July 2020. The outbreak of COVID-19 was declared a public emergency of international concern and a pandemic, respectively, on 30 Jan 2020 and 11 March 2020 by the World Health Organization. Currently, PCR has a 6.3% positive rating across 80 countries. In India, there are 2557 new cases. In some people, vaccine side effects are also detected. The SARS-COV-2, part of the COVID-19 family, is sensitive to ultraviolet rays and heat. These viruses are inactivated for a half-hour at 56^0c and -80^0c and stored for years [23]. The covid 19 is inactivated effectively by 75% ethanol, chlorine, and peracetic acid. Eliminating the source of infections is the primary principle in controlling and preventing disease to protect the sensitive population [23]. In this molecular docking study, fifteen drugs were performed with the therapeutic target of protein of SARS-Cov-2, i.e., non-structural protein 2. The drug-designing process is in silico, which involves the therapeutic target identification and testing of the heterogeneous building of small molecules against it [22]. After that, docking the smaller molecules from the library initiates virtual screening. The chemicals that pass these detailed profiling investigations are referred to as leads. These selected findings are tested for specificity by docking at binding sites of established medication targets [15].

2. MATERIALS AND METHODS

Sequence retrieval

The amino acid sequences of nonstructural protein 2[Accession 7MSW_A] of COVID-19 coronavirus were retrieved from the protein database of the NCBI. The protein is 638 amino acids long and used for further analysis in this current study.

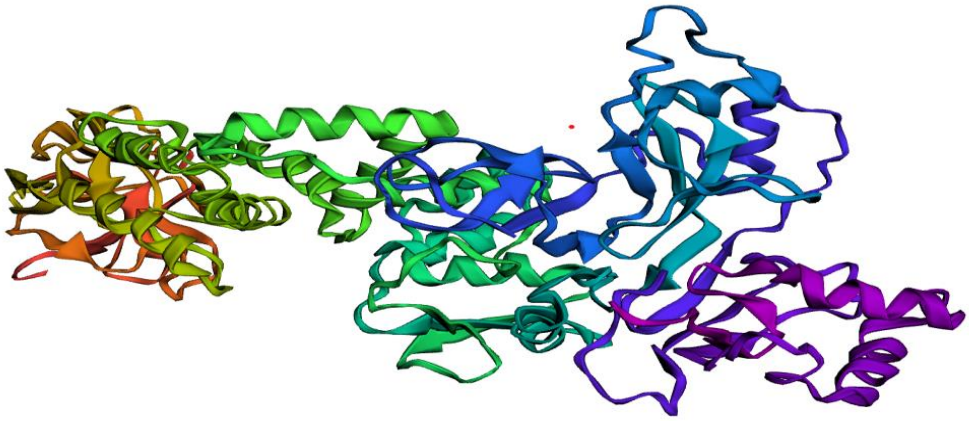

Figure 1: Structure of Nonstructural Protein of Novel Coronavirus

Primary structure prediction

ExPasy's ProtParam tool [10] was utilized to calculate the physicochemical characteristics of the protein. Theoretical isoelectric point (pI), molecular weight, the total number of positive and negative residues, extinction coefficient [18], instability index [19], aliphatic index [22], and grand average hydropathicity (GRAVY) of the protein were calculated using the default parameters.

Table 1: Different Physico-chemical properties of nonstructural protein 2 of coronavirus

Parameters	value
Molecular weight	70511.38
Extinction coefficient Abs 0.1%(=1g/1)1.033, assuming all pairs of Cys residues form cystines	68435
Extinction coefficient Abs 0.1%(=1g/1)1.013, assuming all Cys residues are reduced	66810
Theoretical pI	6.25
Total number of negatively charged residues (Asp + Glu):	74
Total number of positively charged residues (Arg + Lys):	70
Instability index	36.06
Grand average of hydropathicity (GRAVY)	-0.062
Aliphatic index	88.93

Template Selection

BLAST is performed to find a suitable template for the protein. The level of similarity that exists between a protein that has unidentified structures and those that exist within the Protein data bank are shown in Blast results [15]. Through Blast, it was found that the best homolog for Non-structural protein 2 is 7MSW_A with query coverage of 100%. The structural summary for the homology was obtained through PDB. The result of Blast is shown in Figure 2.

Figure 2: non-structural protein 2 Blast

Homology Modeling

The model was generated using a comparative modeling program MODELLER9.20 [3], which produces a refined three-dimensional homology model of a protein sequence based on a given sequence alignment and selected template. Homology modeling can produce high-quality models provided the query and template molecules are closely related. However, model quality can decrease if the target and template sequence identity fall below 20 %. However, it was proved that protein structures are more conserved than their sequences if the identity is > 20 % [34]. The MODELLER generated five structures with 7MSW A as template structures from which the best one is selected based on the lowest Discrete Optimized Protein Energy (DOPE) score and highest GA341 score [16].

Ligand's preparation

Some of the Natural drug molecules and their analogs were taken from the National Centre for Biotechnology Information (NCBI) Pub-Chem compound database as ligand molecules. These molecules were downloaded in Structure Data File (SDF) format and converted to Protein Data Bank (PDB) coordinates using an Open Babel converter. The selected ligand molecules were passed through the Molinspiration server, and the likeliness of the same was checked by Lipinski1s Rule of five to identify their drug-like properties. Only the molecules that passed through this filter were used for further analysis. An ideal drug molecule should have a molecular weight of less than 500, the total number of hydrogen bonds should not exceed 5, the miLogP value should be less than 5, and the sum of N and O should not exceed 10 [31].

Table 2: Molecular Properties of Ligand molecules identified by Molinspiration server

Ligand	miLogP	TPSA	Natoms	MW	nON	NOHNH	n violations	Nrotb	Volume
1	2.85	112.28	36	498.57	8	1	0	6	452.45
2	3.66	86.11	34	466.57	6	0	0	3	430.17
3	1.05	86.99	25	350.45	5	3	0	3	338.33
4	1.38	41.12	16	224.35	3	2	0	4	236.41
5	5.40	110.52	43	596.72	9	0	2	9	551.94
6	0.86	23.55	16	224.35	3	0	0	4	236.69
7	1.72	66.76	24	334.46	4	2	0	4	330.29
8	4.34	95.35	35	485.57	7	0	0	3	439.15
9	1.17	125.69	34	480.60	8	4	0	7	454.37
10	2.04	134.27	34	470.52	8	3	0	4	417.39
11	1.83	100.13	32	442.55	6	3	0	1	408.10
12	3.55	118.36	39	540.61	9	0	1	8	488.96
13	1.94	92.06	34	466.53	7	0	0	4	417.03
14	2.15	175.51	45	632.75	11	5	2	6	574.50
15	4.15	96.36	34	470.61	6	2	0	2	441.81

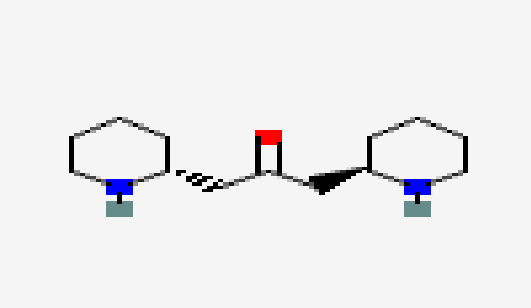

Anaferine

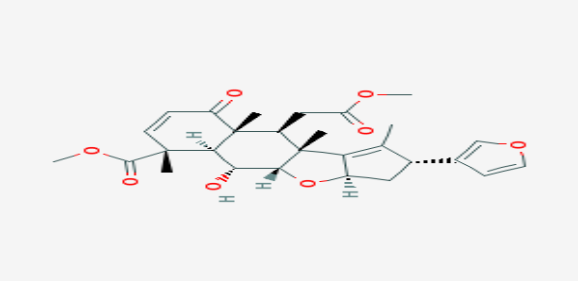

6 Deacetylnimbine

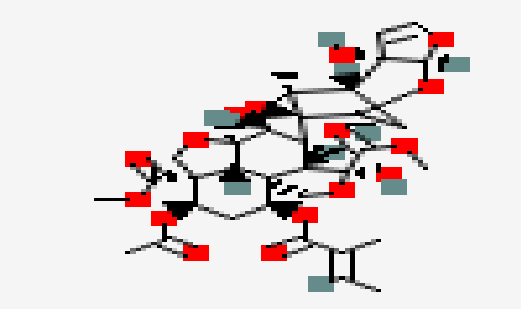

Azadirachtin

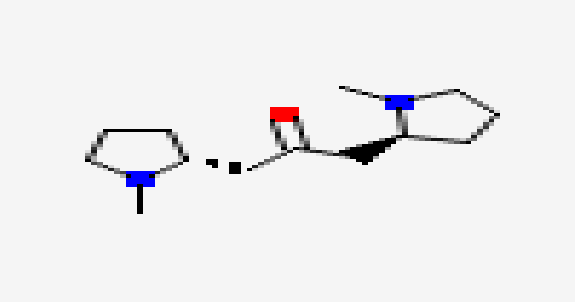

Cuscohygrine

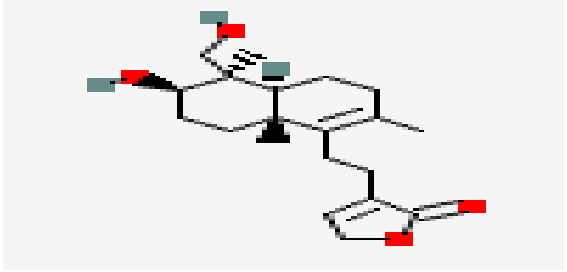

Deoxyandrographolide

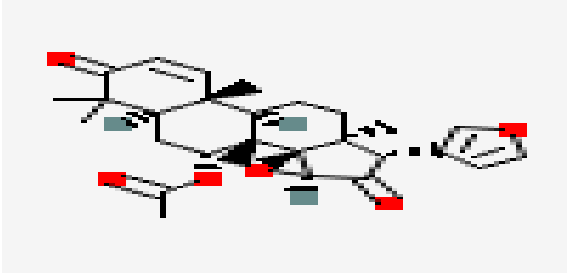

Epoxyazadiradione

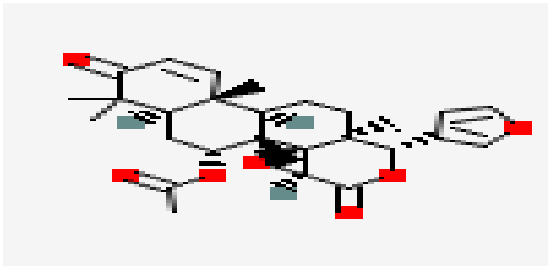

Gedunin

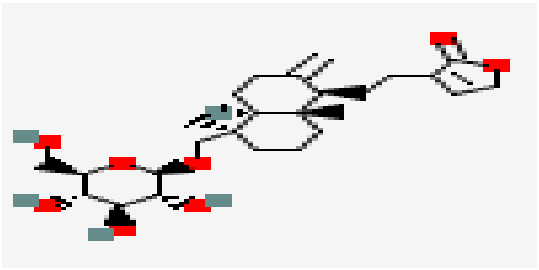

Neoandrographolide

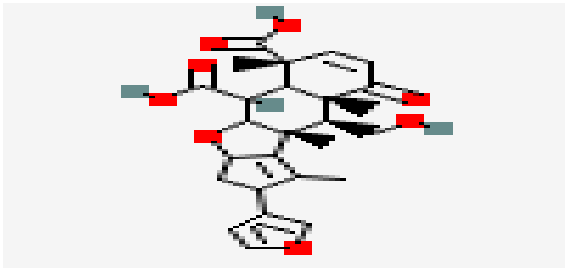

Nimbic acid

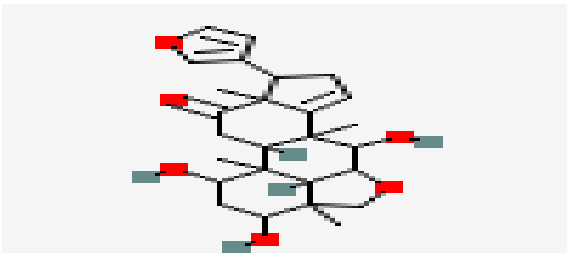

Nimbidinin

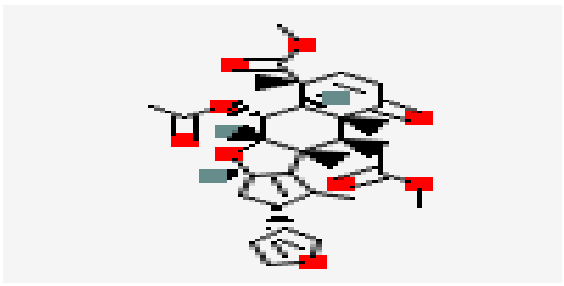

Nimbin

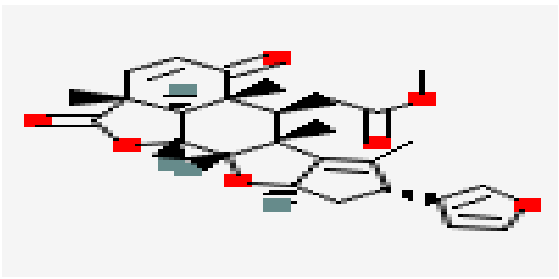

Nimbolide

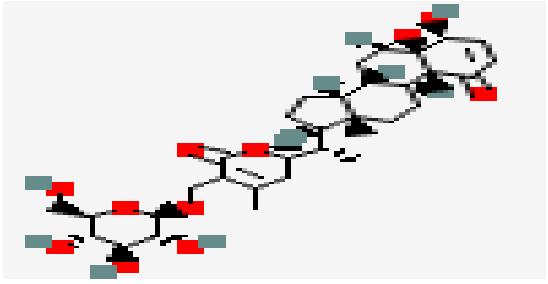

Sitoindosides IX

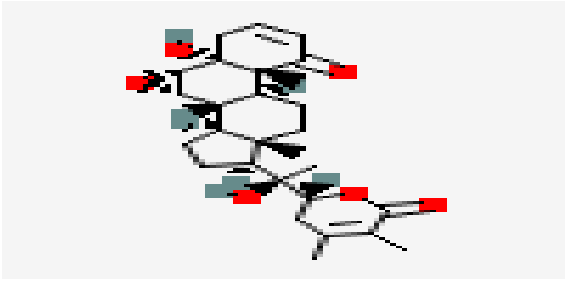

Withanolide A

Verification and validation of the structure

The accuracy and stereochemical features of the predicted model were calculated with PROCHECK [25] by Ramachandran Plot analysis [35], which was done through the SAVESv6.0 server

(servicesn.mbiuda.edu/SAVES/). The best model was selected based on the overall G-factor and the number of residues in the core, allowed, generously allowed, and disallowed regions.

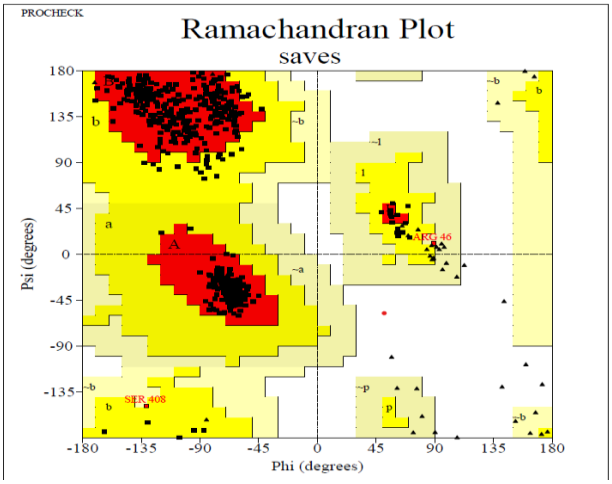

Figure 3: Ramachandran plot analysis of selected model

Table 3: Ramachandran plot of Non-structural protein 2 from *Novel Coronavirus*

Ramachandran plot statistics	Non-structural protein 2	
	Residue	%
Residues in the most favored regions[A,B,L]	525	92.8
Residues in the additional allowed regions [a,b,l,p]	39	6.9
Residues in the generously allowed regions [a,b,l,p]	2	0.4
Residues in the disallowed regions [xx]	0	0.0
Number of non-glycine and non-proline residues	566	100.0
Number of end residues (excl.Gly and PRO)	1	
Number of glycine residues	49	
Number of proline residues	22	
Total number of residues	638	

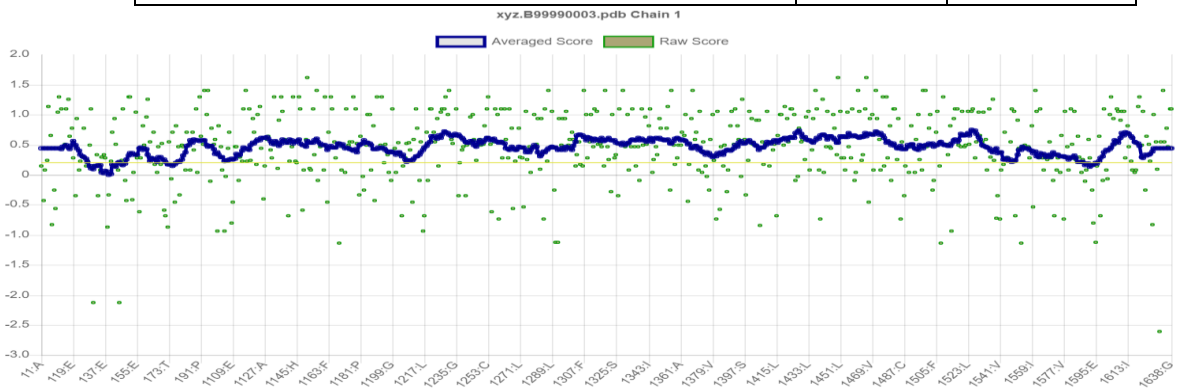

Fig 4: Verify 3D of Non-structural protein 2 of Novel Coronavirus

Active site analysis

After modeling the three-dimensional structure of s Non-structural protein 2, the probable binding sites of the protein were searched based on the structural association of the template and the model constructed with the Computed Atlas of Surface Topography of Proteins (CASTp) server. CASTp3.0 was used to recognize and determine the binding sites, surface structural pockets, active sites, area, shape, and volume of every pocket and internal cavities of proteins. It could also be used to calculate the number, boundary of mouth openings of every pocket, molecular reachable surface, and area [14]. Active site analysis provides significant insight into the docking simulation study.

Docking simulation study

Silico docking simulation study was conducted to recognize the inhibiting potential against non-structural protein 2. The docking study was performed by Autodock Vina and Autodock version 1.5.6. Before starting the docking simulation study, non-structural protein 2 was modified by adding polar hydrogen. All compounds were screened using Autodock Vina version 1.5.6 to search for chemicals with high binding affinities for nonstructural protein 2. The size of the grid box was set as center_x = 109.682, center_y = 115.301, center_z = 125.648, size_x = 78, size_y = 78, size_z = 126. The exhaustiveness level was set to 8. The compound with the highest binding affinities was then analyzed and considered a possible template for further optimization. Then, Autodock version 1.5.6 was performed, and the search results were analyzed using the Lamarckian genetic algorithm. A comparison of ligands is made based on binding energy, and a ligand with minimum binding energy is selected [17].

Table 4: Identifying binding affinity between Protein and ligand by Autodock Vina

Ligand	Binding Affinity	Distance from best mode	
		Msd Lb	Msd Ub
6 desacetyl nimbinene 1	-11.6	0.000	0.000
6 desacetyl nimbinene 2	-10.8	1.266	2.933
Azadirachtin 1	-12.7	0.000	0.000
Azadirachtin 2	-12.5	1.472	5.900
Anaferine 1	-6.7	0.000	0.000
Anaferine 2	-6.7	0.075	4.778
Andrographolide 1	-9.9	0.000	0.000
Andrographolide 2	-9.7	1.130	5.325
Cuscohygrine 1	-7.2	0.000	0.000
Cuscohygrine 2	-7.1	0.740	4.404
Deoxyandrographolode 1	-9.8	0.000	0.000
Deoxyandrographolode 2	-9.3	1.878	5.346
Epoxyazadiradione 1	-14.2	0.000	0.000
Epoxyazadiradione 2	-13.9	1.388	5.825
Gedunin 1	-12.7	0.000	0.000
Gedunin 2	-12.4	1.600	2.953
Neoandrapholide 1	-10.4	0.000	0.000
Neoandrapholide 2	-10.1	16.887	18.510
Nimbic acid 1	-12.3	0.000	0.000
Nimbic acid 2	-12.2	0.735	18.510
Nimbidinin 1	-11.8	0.000	0.000
Nimbidinin 2	-11.7	1.375	5.336
Nimbin 1	-11.1	0.000	0.000
Nimbin 2	-11.0	1.568	3.461
Nimbolide 1	-13.4	0.000	0.000
Nimbolide 2	-13.3	0.751	2.588
Sitoindosides IX 1	-11.4	0.000	0.000
Sitoindosides IX 2	-11.2	19.611	22.787
Withanolides A 1	-11.6	0.000	0.000
Withanolides A 2	-11.4	1.684	6.716

3. RESULTS AND DISCUSSION

The two ligands, namely with epoxyazadiradione -8.4 (BE) and 805.20(IC) and Nimbolide with -10.53 (BE) and 508.16(IC) predicted were highly significant among the 15 ligands with its good binding affinity and inhibition constant. Docking small molecule compounds into a receptor's binding site and estimating the complex's binding affinity is essential to the structure-based drug design process. For a thorough understanding of the structural principles that determine the strength of a protein/ligand complex, an accurate and fast docking protocol & the ability to visualize binding geometries and interactions are mandatory. In the present study, an interface between the popular

molecular graphics system PyMoL1.3 and the molecular docking suites Autodock 1.5.6 and Vina 1.5.6, an attempt was made to demonstrate how the combination of docking and visualization can aid structure-based drug design efforts. In the present work, we describe a plugin for PyMoL1.3 that allows molecular docking, virtual screening, and binding site analysis with PyMoL1.3. The plugin represents an interface between PyMoL1.3 and two popular docking programs, Autodock 1.5.6 and Autodock Vina version 1.5.6, and extensively uses Python script collection to set up docking runs. Since visualization is crucial for structure-based drug design, several tools have been developed to add visual support for the Autodock version 1.5.6 suite. The Visualizer Autodock version 1.5.6 Tools offers a complete molecular viewer and graphical support for all steps required to set up and analyze docking runs. Autodock version 1.5.6 and Vina need receptor and ligand representations in a file format called 'pdbqt,' which is a modified protein data bank format containing atomic charges, atom type definitions, and, for ligands and topological information (rotatable bonds). The plugin executes these file preparations using Autodock version 1.5.6 Tools package scripts. Castp detects pockets and voids in protein structures to determine and characterize binding sites. Ligands for subsequent docking runs can either be prepared one by one through PyMoL1.3 [13] selections or by specifying a directory containing a library of ligands to be docked. Autodock uses interaction maps for docking. Before the docking run, these maps are calculated using the program *autogrid* [21]. For each ligand atom type, the interaction energy between the ligand atom and the receptor is calculated for the entire binding site, which is discretized through a grid. The docking poses are ranked according to their docking scores, and both the ranked list of docked ligands and their corresponding binding poses may be exported. For instance, the ranked list of docking results can be exported in a CSV format and directly imported into programs like Excel.

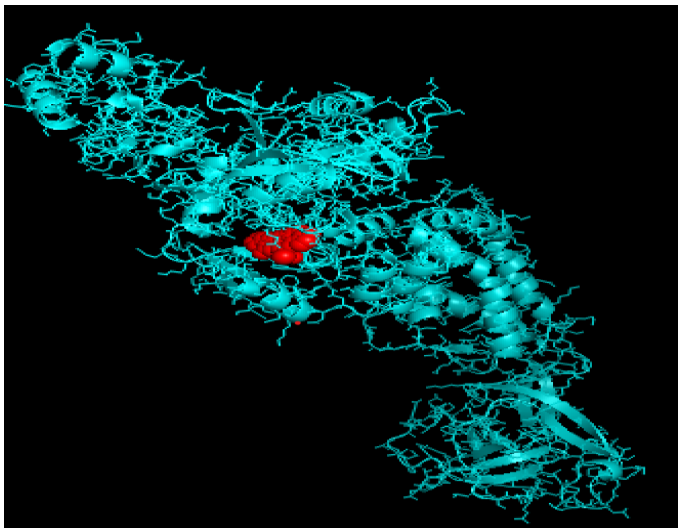

Figure 5: Molecular docking of epoxyazadiradione

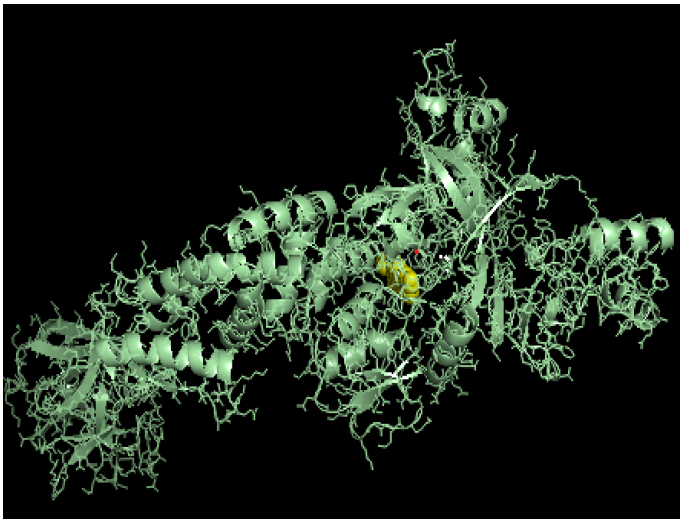

Figure 6: Molecular docking of Nimbolide

Table 5: Identifying binding Energy between Protein and ligand by Autodock

Ligand	Binding Energy	Ligand_ Efficiency	Inhib_ constant	Intermol_ Energy	Vdw_hb_des_ Energy		Total_ internal	Torsional _energy
6 desacetylnimbinene	-7.46	-0.21	3.39 µM	-9.55	-9.55	84.42	2.09	84.42	185.58
Anaferine	-5.02	-0.31	208.6 µM	-6.21	-4.65	18.64	1.19	18.64	199.36
Azadirachtin	-9.91	-0.19	54.68 nM	-13.19	-13.11	159.34	3.28	159.34	183.19
Gedunin	-9.07	-0.26	226.34 nM	-9.96	-9.79	16.43	0.89	16.43	185.64
Cuscohygrine	-5.57	-0.35	82.82 µM	-6.17	-4.27	10.06	0.6	10.06	215.55
Deoxyandrographolode	-6.4	-0.27	20.51 µM	-7.89	-7.56	82.12	1.49	82.12	190.19
Epoxyazadiradione	-8.4	-0.25	805.20 nM	-9.21	9.10	121.01	0.89	120.01	186.33
Neoandrapholide	-7.08	-0.21	6.5 µM	-9.76	-9.73	12.32	2.68	12.32	195.06
Nimbic acid	-9.35	-0.27	140.04 nM	-10.84	-12.31	208.81	1.49	208.81	195.73
Nimbidinin	-10.76	-0.34	12.91 nM	-12.25	-12.24	13.39	1.49	13.39	187.0
Nimbin	-9.08	-0.23	220.67 nM	-11.17	-11.16	109.82	2.09	109.82	186.93
Nimbolide	-10.53	-0.35	508.16 nM	-12.54	-12.44	9.97	0.6	9.97	186.14
Sitoindosides IX	-8.05	-0.18	1.26 µM	-11.33	-11.14	44.27	3.28	44.27	192.88
Withanolides A	-10.01	-0.29	46.12 nM	-10.9	-10.9	54.98	0.89	54.98	186.53
Andrographolide	-9.77	-0.39	69.41 nM	-10.96	-10.94	10.14	1.19	10.14	187.05

4. CONCLUSION

In the present study, a novel plugin was proposed for the popular molecular graphics system PyMoL1.3, which allows docking studies to be performed using Autodock version 1.5.6 or Autodock/Vina v1.5.6. The plugin covers all functionalities for the entire workflow of a docking run, plus additional functionality to prepare, execute, and analyze virtual screening tasks. Since visual support is essential to structure-based drug design, the plugin is expected to enhance these efforts by combining two widely used docking programs and PyMoL1.3. Fifteen compounds were found in the different articles that inhibited *covid-19 coronavirus* in the Invitro drug susceptibility assay. Globally, one vaccine, Covax, is available, and there are some non-approved drugs. The COVID-19 coronavirus merged in 2019 in China, and the pandemic threatens global health worldwide. This study aimed to examine some drugs that may inhibit the COVID-19 non-structural protein 2, which is used to bond with the human prohibitin receptor. The established ligand-based pharmacophore model was used to identify the common features of non-structural protein 2 inhibitors from the PubChem database, and the virtual screening method was used to screen the library of compounds. After that, molecular docking was employed to study the detailed binding mode between the selected ligands and the active site of non-structural protein 2. The computational approaches showed the advantage of saving time and resources. It is feasible to block the interaction of non-structural protein 2 from the selected 15 compounds using virtual screening based on pharmacophore and molecular docking studies. Several active compounds that are structurally diverse were identified in non-structural protein 2 inhibitors of *covid 19 coronavirus*. This revealed that sequential use of the available tools, such as Autodock/Vina, yields better results in blocking the interaction of non-structural protein 2. In the following study, two chemical compounds, epoxyazadiradione and Nimbolide, were predicted. These compounds hit by the pharmacophore model, virtual screening, and molecular docking need further verification using related biological experiments. Such further studies may help to find effective inhibitors of non-structural protein 2 of the virus; due to this, there will be no interaction with the human Prohibitin receptor.

ETHICS APPROVAL AND CONSENT TO PARTICIPATE

Not applicable.

HUMAN AND ANIMAL RIGHTS

No animals or humans were used for the studies that are based on this research.

CONSENT FOR PUBLICATION

Not applicable.

FUNDING

None.

ACKNOWLEDGEMENT

I thank all those people who have supported in this research work.

CONFLICT OF INTEREST

I declare that there is no conflict of interest

REFERENCES

1. Abd El-Aziz TM, Stockand JD. Recent progress and challenges in drug development against COVID-19 coronavirus (SARS-CoV-2)-an update on the status. Infection, Genetics and evolution. 2020 Sep 1;83:104327.
2. Ahmad S, Bhanu P, Kumar J, Pathak RK, Mallick D, Uttarkar A, Niranjan V, Mishra V. Molecular dynamics simulation and docking studies reveal NF-κB as a promising therapeutic drug target for COVID-19.
3. Al-Karmalawy AA, Alnajjar R, Dahab M, Metwaly A, Eissa I. Molecular docking and dynamics simulations reveal the potential of anti-HCV drugs to inhibit COVID-19 main protease. Pharmaceutical Sciences. 2021 Jan 29;27(Covid-19):S109-21.
4. Alnajjar R, Mostafa A, Kandeil A, Al-Karmalawy AA. Molecular docking, molecular dynamics, and in vitro studies reveal the potential of angiotensin II receptor blockers to inhibit the COVID-19 main protease. Heliyon. 2020 Dec 1;6(12).
5. Angelini MM, Akhlaghpour M, Neuman BW, Buchmeier MJ. Severe acute respiratory syndrome coronavirus nonstructural proteins 3, 4, and 6 induce double-membrane vesicles. MBio. 2013 Aug 30;4(4):10-128.
6. Asselah T, Durantel D, Pasmant E, Lau G, Schinazi RF. COVID-19: Discovery, diagnostics and drug development. Journal of hepatology. 2021 Jan 1;74(1):168-84.
7. Badam L, Joshi SP, Bedekar SS. 'In vitro'antiviral activity of neem (Azadirachta indica. A. Juss) leaf extract against group B coxsackieviruses. The Journal of communicable diseases. 1999 Jun 1;31(2):79-90.
8. Chothia C, Lesk AM. The relation between the divergence of sequence and structure in proteins. The EMBO journal. 1986 Apr 1;5(4):823-6.
9. Clark LK, Green TJ, Petit CM. Structure of nonstructural protein 1 from SARS-CoV-2. Journal of Virology. 2021 Jan 28;95(4):10-128.
10. Colovos C, Yeates TO. Verification of protein structures: patterns of nonbonded atomic interactions. Protein science. 1993 Sep;2(9):1511-9.
11. Cornillez-Ty CT, Liao L, Yates III JR, Kuhn P, Buchmeier MJ. Severe acute respiratory syndrome coronavirus nonstructural protein 2 interacts with a host protein complex involved in

mitochondrial biogenesis and intracellular signaling. Journal of virology. 2009 Oct 1;83(19):10314-8.

12. da Silva SJ, da Silva CT, Mendes RP, Pena L. Role of nonstructural proteins in the pathogenesis of SARS-CoV-2. Journal of medical virology. 2020 Sep;92(9):1427.
13. DeLano WL. CCP4 Newsletter on protein crystallography. The PyMOL molecular graphics system. 2002:44-53.
14. Dundas J, Ouyang Z, Tseng J, Binkowski A, Turpaz Y, Liang J. CASTp: computed atlas of surface topography of proteins with structural and topographical mapping of functionally annotated residues. Nucleic acids research. 2006 Jul 1;34(suppl_2):W116-8.
15. Ekenna C, Fatumo S, Adebiyi E. In-silico evaluation of malaria drug targets. International Journal of Engineering and Technology. 2010 Apr 1;2(2):132.
16. Eswar N, Webb B, Marti-Renom MA, Madhusudhan MS, Eramian D, Shen MY, Pieper U, Sali A. Comparative protein structure modeling using Modeller. Curr. Protoc. Bioinformatics Chapter 5. Unit. 2006;5:6.
17. Ferreira LG, Dos Santos RN, Oliva G, Andricopulo AD. Molecular docking and structure-based drug design strategies. Molecules. 2015 Jul 22;20(7):13384-421.
18. Gill SC, Von Hippel PH. Calculation of protein extinction coefficients from amino acid sequence data. Analytical biochemistry. 1989 Nov 1;182(2):319-26.
19. Guruprasad K, Reddy BB, Pandit MW. Correlation between stability of a protein and its dipeptide composition: a novel approach for predicting in vivo stability of a protein from its primary sequence. Protein Engineering, Design and Selection. 1990 Dec 1;4(2):155-61.
20. Hagar M, Ahmed HA, Aljohani G, Alhaddad OA. Investigation of some antiviral N-heterocycles as COVID 19 drug: molecular docking and DFT calculations. International Journal of Molecular Sciences. 2020 May 30;21(11):3922.
21. http://autodock.scripps.edu/faqs-help/how-to/how-to-prepare-a-grid-parameter-files-for-autogrid4
22. Ikai A. Thermostability and aliphatic index of globular proteins. The Journal of Biochemistry. 1980 Oct 1;88(6):1895-8.
23. Keretsu S, Bhujbal SP, Cho SJ. Rational approach toward COVID-19 main protease inhibitors via molecular docking, molecular dynamics simulation and free energy calculation. Scientific reports. 2020 Oct 19;10(1):17716.
24. Kumar CS. An insight to drug designing by in-silico approach in biomedical research. J Pub Health Med Res. 2013;1(2):63-5.

25. Laskowski RA, Rullmann JA, MacArthur MW, Kaptein R, Thornton JM. AQUA and PROCHECK-NMR: programs for checking the quality of protein structures solved by NMR. Journal of biomolecular NMR. 1996 Dec;8:477-86.
26. Mei M, Tan X. Current strategies of antiviral drug discovery for COVID-19. Frontiers in Molecular Biosciences. 2021 May 13;8:671263.
27. Muratov EN, Amaro R, Andrade CH, Brown N, Ekins S, Fourches D, Isayev O, Kozakov D, Medina-Franco JL, Merz KM, Oprea TI. A critical overview of computational approaches employed for COVID-19 drug discovery. Chemical Society Reviews. 2021;50(16):9121-51.
28. Miller LH, Ackerman HC, Su XZ, Wellems TE. Malaria biology and disease pathogenesis: insights for new treatments. Nature medicine. 2013 Feb;19(2):156-67.
29. Modeller N, Eswar MA, Marti Renom B. Comparative protein structure modeling with modeller. Current Protocols in Bioinformatics, John Wiley & Sons, Inc., Supplement. 2006;15(5.6):1-5.
30. Muratov EN, Amaro R, Andrade CH, Brown N, Ekins S, Fourches D, Isayev O, Kozakov D, Medina-Franco JL, Merz KM, Oprea TI. A critical overview of computational approaches employed for COVID-19 drug discovery. Chemical Society Reviews. 2021;50(16):9121-5
31. Narayanaswamy R, Lam KW, Ismail IS. Molecular docking analysis of natural compounds as Human neutrophil elastase (HNE) inhibitors. J Chem Pharm Res. 2013;5:337-41.
32. Rani I, Kalsi A, Kaur G, Sharma P, Gupta S, Gautam RK, Chopra H, Bibi S, Ahmad SU, Singh I, Dhawan M. Modern drug discovery applications for the identification of novel candidates for COVID-19 infections. Annals of Medicine and Surgery. 2022 Aug 1;80:104125.
33. Rohaim MA, El Naggar RF, Clayton E, Munir M. Structural and functional insights into non-structural proteins of coronaviruses. Microbial pathogenesis. 2021 Jan 1;150:104641.
34. Šali A, Blundell TL. Comparative protein modelling by satisfaction of spatial restraints. Journal of molecular biology. 1993 Dec 5;234(3):779-815.
35. Sasisekharan RG. Stereochemistry of polypeptide chain configurations J Mol Biol 79599. Ramachandran GN, Ramakrishnan C, and Sasisekharan (1963). Stereochemistry of polypeptide chain configurations. J Mol Biol. 1963;7:95-9.
36. Wadood A, Ahmed N, Shah L, Ahmad A, Hassan H, Shams SJ. In-silico drug design: An approach which revolutionarised the drug discovery process. OA Drug Des Deliv. 2013 Sep 1;1(1):3.
37. World Health Organization. COVID-19 weekly epidemiological update, 9 March 2021.
38. Yadav R, Chaudhary JK, Jain N, Chaudhary PK, Khanra S, Dhamija P, Sharma A, Kumar A, Handu S. Role of structural and non-structural proteins and therapeutic targets of SARS-CoV-2 for COVID-19. Cells. 2021 Apr;10(4):821.

39. Yang P, Wang X. COVID-19: a new challenge for human beings. Cellular & molecular immunology. 2020 May;17(5):555-7.
40. Yoshimoto FK. A biochemical perspective of the nonstructural proteins (NSPs) and the spike protein of SARS CoV-2. The protein journal. 2021 Jun;40(3):260-95.
41. Zhou P, Yang XL, Wang XG, Hu B, Zhang L, Zhang W, Si HR, Zhu Y, Li B, Huang CL, Chen HD. A pneumonia outbreak associated with a new coronavirus of probable bat origin. nature. 2020 Mar;579(7798):270-3.